SOCIETY

British Journal of Pharmacology (2010), 159, 176–187

0007-1188/09
www.brjpharmacol.org

RESEARCH PAPER

Pharmacokinetic–pharmacodynamic modelling of the analgesic effects of lumiracoxib, a selective inhibitor of cyclooxygenase-2, in rats

DA Vásquez-Bahena[1], UE Salazar-Morales[1], MI Ortiz[2], G Castañeda-Hernández[1] and IF Trocóniz[3]

[1]*Sección Externa de Farmacología, Centro de Investigación y de Estudios Avanzados del Instituto Politécnico Nacional, Mexico City, Mexico,* [2]*Área Académica de Medicina del Instituto de Ciencias de la Salud, Universidad Autónoma del Estado de Hidalgo, Pachuca, Hidalgo, Mexico, and* [3]*Department of Pharmacy and Pharmaceutical Technology, Faculty of Pharmacy, University of Navarra, Pamplona, Spain*

Background and purpose: This study establishes a pharmacokinetic/pharmacodynamic (PK/PD) model to describe the time course and *in vivo* mechanisms of action of the antinociceptive effects of lumiracoxib, evaluated by the thermal hyperalgesia test in rats.

Experimental approach: Female Wistar fasted rats were injected s.c. with saline or carrageenan in the right hind paw, followed by either 0, 1, 3, 10 or 30 mg·kg^{-1} of oral lumiracoxib at the time of carrageenan injection (experiment I), or 0, 10 or 30 mg·kg^{-1} oral lumiracoxib at 4 h after carrageenan injection (experiment II). Antihyperalgesic responses were measured as latency time (LT) to a thermal stimulus. PK/PD modelling of the antinociceptive response was performed using the population approach with NONMEM VI.

Results: A two-compartment model described the plasma disposition. A first-order model, including lag time and decreased relative bioavailability as a function of the dose, described the absorption process. The response model was: $LT = LT_0/(1 + MED)$. LT_0 is the baseline response, and *MED* represents the level of inflammatory mediators. The time course of MED was assumed to be equivalent to the predicted profile of COX-2 activity and was modelled according to an indirect response model with a time variant synthesis rate. Drug effects were described as a reversible inhibition of the COX-2 activity. The *in vivo* estimate of the dissociation equilibrium constant of the COX-2-lumiracoxib complex was 0.24 μg·mL^{-1}.

Conclusions: The model developed appropriately described the time course of pharmacological responses to lumiracoxib, in terms of its mechanism of action and pharmacokinetics.

British Journal of Pharmacology (2010) **159,** 176–187; doi:10.1111/j.1476-5381.2009.00508.x; published online 2 December 2009

Keywords: pharmacokinetic/pharmacodynamic modelling; cyclooxygenase-2; inflammatory mediators; hyperalgesia; time latency

Abbreviations: C_{MAX}, maximum plasma concentration; COX, cyclooxygenase; COX-2, cyclooxygenase-2; C_p, plasma concentration; IIV, interindividual variability; K_D, equilibrium dissociation constant of the COX-2-C_P complex; $k_{D\_COX\text{-}2}$, first-order rate constant of degradation of COX-2; $k_{S\_COX\text{-}2(t)}$, time variant zero-order rate constant of synthesis of COX-2; LT, latency time; LT_0, latency time at baseline; MED, inflammatory mediators; NSAID, non-steroidal anti-inflammatory drug; PK/PD, pharmacokinetic/pharmacodynamic; Red_{MAX}, maximum percentage reduction in latency response with respect to baseline

Introduction

Classical non-steroidal anti-inflammatory drugs (NSAIDs) are the mainstay of therapy for several diseases associated with inflammation and pain, such as osteoarthritis and rheumatoid arthritis. Notwithstanding, their long-term use is associated with gastrointestinal ulceration and serious gastrointestinal complications, such as perforation and bleeding (Hernández-Díaz and García-Rodríguez, 2001). It has been proposed that NSAIDs-induced gastrointestinal damage involves local inhibition of the cyclooxygenase-1 (COX-1) enzyme, which generates cytoprotective prostaglandins in the gastrointestinal tract (Crofford, 1997; Warner *et al.*, 1999). The identification of a second isoform of the cyclooxygenase enzyme, COX-2, which is up-regulated as a result of

Correspondence: Dr. Iñaki F Trocóniz, Departamento de Farmacia y Tecnología Farmacéutica, Facultad de Farmacia, Universidad de Navarra, Pamplona 31080, Spain. E-mail: itroconiz@unav.es
Received 3 April 2009; revised 29 July 2009; accepted 30 July 2009

inflammation (Fu *et al.*, 1990), provided the impetus for the development of COX-2 selective inhibitors. Selective inhibitors of the COX-2 enzyme, referred to as coxibs, were developed as analgesic and anti-inflammatory agents with significantly less gastrointestinal toxicity compared with traditional NSAIDs (Bombardier *et al.*, 2000; Goldstein *et al.*, 2001). Lumiracoxib is the most selective COX-2 inhibitor available that has been tested clinically. The relative potency ratios (COX-2/COX-1) are 433, 344, 272 and 30 for lumiracoxib, etoricoxib, rofecoxib and celecoxib respectively (Shi and Klotz, 2008). Unlike other COX-2 inhibitors, which contain a sulphone group or a sulphonamide group, lumiracoxib possesses a carboxylic acid group, making it weakly acidic (Rordorf *et al.*, 2005).

As a result of its chemical structure, lumiracoxib exhibits moderate clearance. Despite its short half-life (5–8 h), lumiracoxib is given once daily (Mysler, 2004), suggesting a different pharmacokinetic/pharmacodynamic (PK/PD) relationship as compared with other coxibs. Half-life values for etoricoxib, rofecoxib and celecoxib are 11–16, ~17 and 19–32 h respectively (Ahuja *et al.*, 2003; Shi and Klotz, 2008). Celecoxib is given twice daily, while rofecoxib and etoricoxib are given once daily.

There is evidence that lumiracoxib is effective in the treatment of osteoarthritis, rheumatoid arthritis and acute pain (Rordorf *et al.*, 2005). The onset of lumiracoxib analgesia in post-operative dental pain is faster than for other coxibs, although the rate of absorption is similar (Ahuja *et al.*, 2003; Shi and Klotz, 2008). Pain intensity differences were significantly different from placebo at 15, 30 and 60 min for lumiracoxib, rofecoxib and celecoxib respectively (Kellstein *et al.*, 2004). On the other hand, there is evidence that lumiracoxib is readily transferred to inflamed tissues (Weaver *et al.*, 2003). Thus, it appears that the rapid onset of action of lumiracoxib is due to a rapid distribution to its effect compartment, rather than to a rapid absorption. It has been also observed that lumiracoxib accumulates in inflamed tissues, having a residence time longer than in plasma allowing a once-daily dosing (Scott *et al.*, 2004).

PK/PD modelling represents a powerful tool to understand the *in vivo* time course of pharmacological effects, providing insight on the mechanisms of action through the quantitative description of the pharmacokinetic, pharmacodynamic and system-related processes (Giraudel *et al.*, 2005). Despite a large body of scientific literature on the pharmacokinetics and pharmacodynamics of NSAIDs, information on the integrated pharmacokinetic–pharmacodynamic profile of these agents is sparse (Castañeda-Hernández *et al.*, 1995; Flores-Murrieta *et al.*, 1998; Josa *et al.*, 2001; Huntjens *et al.*, 2005). Furthermore, to our knowledge, for the particular case of coxibs, there is a lack of studies dealing with the *in vivo* analysis of concentration-effect relationships.

Several coxibs have been withdrawn from the market due to unexpected side effects, including cardiovascular and hepatic damage. It has been pointed out, however, that such withdrawals were due to lack of information on PK/PD relationships during the development and assessment of the rationale for dose selection, which was based on symptomatic relief rather than on understanding of the degree of COX blockade required to yield analgesia (Hinz and Brune, 2008).

On the basis of such considerations, the objective of the current study was to establish a PK/PD model for the analgesic effects of lumiracoxib in the rat, identifying the rate-limiting steps in the time course of the response to lumiracoxib, and characterizing the *in vivo* concentration-response relationship. To achieve our purpose, we used the thermal hyperalgesia test, which has been shown to be a reliable model for the quantitative assessment of inflammation-induced nociception (Hargreaves *et al.*, 1988). We adapted the assay in order to determine nociception and plasma concentrations in the same animal, thus allowing characterization of the individual PK/PD relationship.

Methods

Animals

All animal care and experimental procedures followed the Guidelines on Ethical Standards for Investigation of Experimental Pain in Animals (Zimmermann, 1983), and the protocol was approved by the Institutional Animal Care and Use Committee (Centro de Investigación y de Estudios Avanzados del Instituto Politécnico Nacional, Mexico City, Mexico). Female Wistar rats, weighing 180–200 g, were used in this study. Food was withdrawn 12 h before initiation of experiments, but animals had free access to drinking water. At the end of the experiments, rats were killed in a CO_2 chamber.

Study design

The current study involved two experiments. Briefly, the data collected in experiment II were used mainly to validate externally the PK/PD model developed with the data obtained from experiment I.

Experiment I. Sixty female rats were randomly allocated to six groups. At the start of the experiment, group I received a single intraplantar injection of saline solution 0.9% (100 μL) in the right hind paw, whereas animals in groups II–VI received a single intraplantar injection of a 1% carrageenan suspension in 0.9% saline (100 μL). In addition, animals in groups III–VI were given lumiracoxib orally at the following doses 1 $mg \cdot kg^{-1}$ (group III), 3 $mg \cdot kg^{-1}$ (group IV), 10 $mg \cdot kg^{-1}$ (group V) or 30 $mg \cdot kg^{-1}$ (group VI), immediately after the carrageenan injection. Lumiracoxib was suspended in 0.5% carboxymethyl cellulose solution and Tween 80 and given in a volume equal to 4 $mL \cdot kg^{-1}$.

Blood samples of 200 μL were drawn by means of a cannula inserted in the caudal artery as previously described (Cruz *et al.*, 2002). The cannula was inserted 1 h before experiments. Animals were kept restrained between measurements of hyperalgesia to avoid movement resulting in the removal of the cannula. Samples were collected at the following times after drug administration: 0.083, 0.16, 0.25, 0.33, 0.5, 0.75, 1, 2, 3, 4, 6, 8 and 10 h. Each animal contributed four or five blood samples, taken at times covering uniformly the 10 h experiment period. A 10 h observation period was chosen on the basis of pilot experiments and previous pharmacokinetic data on lumiracoxib pharmacokinetics in the rat (Esser *et al.*,

2005a). On the other hand, the antihyperalgesic response could be reliably followed during 10 h under these experimental conditions.

Lumiracoxib concentrations in plasma and pharmacological response were determined as described below. Measurements of the antihyperalgesic effect of lumiracoxib were performed in the same animals before and 1, 2, 3, 4, 5, 6, 8 and 10 h after saline or carrageenan injection. The pharmacological response was determined as described below.

Experiment II. Twenty female rats were divided at random in three groups. At the start of the experiment, rats received a single injection of carrageenan as it was described for experiment I. Then, animals received oral vehicle (group VII) or lumiracoxib at either 10 mg·kg^{-1} (group VIII) or 30 mg·kg^{-1} (group IX) 4 h after the injection of carrageenan. Measurements of the antihyperalgesic effect were made before and 1, 2, 3, 4, 5, 6, 7, 8, 9, 10, 11, 12, 16, 20 and 24 h after carrageenan injection for each animal.

To summarize the main differences in the experimental design between experiment I and II: (i) Lumiracoxib was administered before (experiment I) and during (experiment II) the development of inflammation, (ii) pharmacokinetics of lumiracoxib was not studied in experiment II, and (iii) the period for latency measurement was expanded to 24 h in experiment II.

Measurement of antinociceptive activity

The animal model of thermal hyperalgesia (Hargreaves *et al.*, 1988) was used to evaluate the pharmacological effect of lumiracoxib. A plantar test (Ugo Basile apparatus, Linton Instrumentation, Comerio, Italy) was used to measure the withdrawal latencies of the hind paw from a radiant heat stimulus. Thirty minutes before the start of the experiments, animals were placed individually in traps to acclimatize them to the testing environment. Animals were manually placed on the glass surface, leaving the hind paws uncovered. The thermal nociceptive stimulus originated from a high-intensity projector lamp bulb (infrared intensity: 217 mW·cm^{-2}) was manually manipulated and positioned under the footpad before and after the plantar injection of saline or carrageenan into the right hind paw. It has been demonstrated that lumiracoxib, at the doses used in this study, does not produce any motor impairment that can interfere with the assay (Ortiz and Castañeda-Hernández, 2008). The paw withdrawal latency time (LT), defined as the time required for the paw to show an abrupt withdrawal, was recorded. In all cases, a cut-off of 30 s was employed to avoid tissue injury.

Analysis of lumiracoxib in plasma

Blood samples were collected in heparinized tubes and centrifuged at 12 400× *g* for 10 min. Plasma samples (100 μL) were separated and frozen at −70°C until analysis. Lumiracoxib concentrations in plasma were determined by high-performance liquid chromatography using ultra violet detection. The analytical method was developed and validated previously at the laboratory (data not published). Briefly, 75 μL of internal standard (30 μg naproxen·mL^{-1} methanol) was added to 100 μL of plasma, and 825 μL of methanol was added to extract the drug by vortex agitation during 5 min at maximum speed, then samples were centrifuged at 12 400× *g* during 10 min. An aliquot (60 μL) was injected into the chromatographic system equipped with a Novapak C-18 column (150_3.9 mm ID, particle size 4 mm, Waters Assoc., Milford, MA, USA) eluted with a mobile phase consisting of a mixture of acetate buffer (0.035M; pH 3.3) with methanol (62:38 v·v^{-1}) at constant flow (1.0 mL·min^{-1}) at room temperature. The effluent from the column was monitored spectrophotometrically at a wavelength 270 nm. Under these conditions, the naproxen and lumiracoxib were eluted at retention times 3.21 and 8.34 min respectively. The limit of detection was 0.06 μg·mL^{-1}, and the quantification limit was 0.10 μg·mL^{-1}. The method was linear in the range of 0.1–8.0 μg·mL^{-1} (r^2 of 0.9996). At concentrations of 0.2, 2 and 7 μg·mL^{-1}, the coefficient of variability was less than 5% for lumiracoxib.

Data analysis

The time course of LT response was described by a model integrating the pharmacokinetics and pharmacodynamic properties of lumiracoxib and the progression of the inflammatory response induced by the injection of carrageenan.

The data were analysed based on the population approach (Beal and Sheiner, 1982; Sheiner and Ludden, 1992) using the first-order conditional estimation method with the INTERACTION option implemented in the software NONMEM (ICON, Ellicott City, MD, USA) version VI (Beal and Sheiner, 1989–2006).

Inter-individual variability (IIV) was modelled exponentially and expressed as coefficient of variation [CV (%)]. Intra-individual (residual) variability for the case of the plasma concentration of lumiracoxib (C_P) was described with a combined error model, and in the case of the analysis of the LT response, an additive error model was used.

Model selection was based on a number of criteria, such as the exploratory analysis of the goodness-of-fit plots performed with Xpose version 4 (University of Uppsala, Uppsala, Sweden; Jonsson and Karlsson, 1999) programmed in the statistics package R, the precision of model parameter estimates represented by the coefficient of variation [CV (%)], computed as the ratio between the standard error provided by NONMEM and the parameter estimate, and multiplied by 100, and the minimum value of the objective function (MOFV) provided by NONMEM. The difference in the MOFV between two hierarchical models was compared with a χ^2 distribution in which a difference of 6.63 points is significant at the 1% level for one extra parameter.

The final models were further evaluated using visual predictive (visual and numerical) checks. Visual predictive check (Karlsson and Holford, 2008): For each type of measurement (C_P or LT) and experimental group, 1000 time profiles were simulated using the selected models and the corresponding parameter estimates. The 2.5, 50, and 97.5th percentiles were then calculated, and the agreement between simulations and raw data was inspected visually. Numerical predictive check: 1000 datasets having the same characteristics as the original dataset were simulated, and for each dataset, the mean C_{MAX}, maximum concentration of lumiracoxib in plasma, AUC_{0-last},

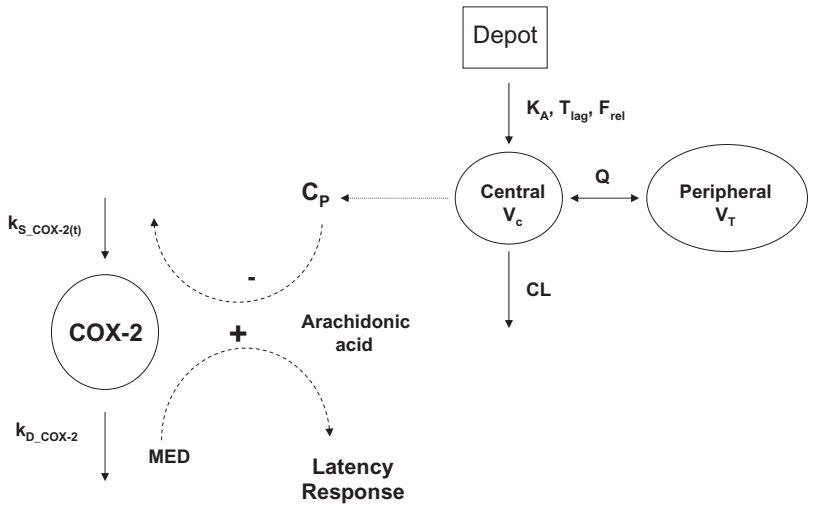

Figure 1 Schematic representation of the PK/PD model selected to describe the data for experiments I and II. C_P, concentration of lumiracoxib in plasma; COX-2, arbitrary levels of active COX-2; F_{rel}, relative bioavailability; K_A, first-order rate constant of absorption; k_{D_COX-2}, first-order rate constant of degradation of COX-2; k_{S_COX-2}, time variant zero-order rate constant of synthesis of COX-2; PK/PD, pharmacokinetic/pharmacodynamic T_{lag}, lag time; MED, inflammatory mediators; Q, and CL, inter-compartmental and elimination clearances respectively; V_c and V_T, apparent volumes of distribution in the central and peripheral compartments respectively.

the area under the plasma concentration versus time curve from time 0 to the last pharmacokinetic measurement, LT_{min}, minimum value of LT response, and Red_{MAX} (%), percentage of maximum reduction in LT with respect to LT_0, were computed. Then, the 2.5th and 97.5th percentile and the overall mean computed from the 1000 simulated studies were calculated and compared with the same descriptors calculated from the raw data.

Graphical summaries and simulations were performed in S-PLUS 6.2. professional edition software (Copyright 1988, 2002 Insightful Corp., Seattle, WA, USA).

Pharmacokinetic modelling. The pharmacokinetics of lumiracoxib in plasma was described by compartmental models parameterized in terms of an apparent volume of distribution, inter-compartmental clearance, and total clearance. Different models were also fitted to the data to characterize the absorption process: zero and first order rate models, with or without the presence of a lag time. The effect of the dose was explored in all the pharmacokinetic parameters, including relative bioavailability (F_{rel}) (Josa *et al*., 2001).

Pharmacokinetic/pharmacodynamic modelling. The different models fitted to the LT response versus time data are described in the results section. Here we focus on the description of the final selected model, which appears schematically in Figure 1.

The model has the following general form:

$$LT_t = \frac{LT_0}{1 + MED_t} \quad (1)$$

where LT_t is the latency response at time t, LT_0, is the baseline LT, and MED_t, corresponds to the unobserved level of inflammatory mediators in the damaged tissue as a consequence of the presence of the enzyme COX-2 in its active form ($COX\text{-}2_{\_act}$; see below in equation 4). The initial condition for *MED* is 0, and consequently, at the start of the experiment, $LT = LT_0$. An increment in MED_t will lead to a decrease in LT reflecting the phenomena of hyperalgesia.

The time course of (unobserved) COX-2 was modelled as follows:

$$\frac{d\text{COX-2}}{dt} = k_{S\_COX-2(t)} - k_{D\_COX-2} \times \text{COX-2} \quad (2)$$

where $dCOX\text{-}2/dt$ is the rate of change of the enzyme COX-2, $k_{S\_COX-2_{(t)}}$ and k_{D_COX-2} represent the synthesis and degradation processes of the enzyme COX-2 respectively (Dayneka *et al*., 1993). At the start of the study, COX-2 and $k_{S\_COX-2_{(t)}}$ were assumed to be 0. Such an assumption is based on published data where the expression of COX-2 protein and prostaglandin E_2 (PGE) peripheral tissue levels before an inflammatory stimulus was found to be less than 1% compared with post-inflammation (Nantel *et al*., 1999).

The synthesis of COX-2 induced by the injection of carrageenan was not assumed to be constant over the period of the study. Accordingly, different models accounting for a linear or a non-linear increase or decrease in $k_{S\_COX-2_{(t)}}$ with time were fit to the data. In particular, a gamma function (Wise, 1985; Giraudel *et al*., 2005) was explored to describe the time course of $k_{S\_COX-2_{(t)}}$:

$$k_{S\_COX-2_{(t)}} = A \times \alpha^t \times e^{-\beta \times t} \quad (3)$$

where A, α and β are the parameters of the gamma function describing the time course and intensity of the COX-2 synthesis rate.

Drug effects were incorporated in the model assuming that lumiracoxib reversibly blocks (inactivates) COX-2, preventing MED recruitment, and therefore reversing hyperalgesia:

$$\text{COX-2}_{act} = \frac{K_D \times \text{COX-2}}{K_D + C_P} \quad (4)$$

K_D is the equilibrium dissociation constant of the COX-2-C_P complex ($COX\text{-}2_{\_inactive}$). In equation (4), the total plasma

concentrations of lumiracoxib are used and the free fraction is not considered. It is assumed that between arachidonic acid and lumiracoxib, a competitive interaction occurs, and that the concentration of arachidonic acid in the effect site remains unchanged during the study.

Assuming that $COX\text{-}2_{\_inactive} = COX\text{-}2 - COX\text{-}2_{\_act}$, equation (4) is derived after rearrangement of the terms presented previously.

In absence of lumiracoxib, all COX-2 synthesized is in the activated form [$COX\text{-}2_{\_act} = COX\text{-}2$]. In equation (4), C_P represents the predicted plasma level provided by the selected population pharmacokinetic model.

Finally, in equation (1), the time course of MED has been assumed to be identical to the time course of $COX\text{-}2_{\_act}$. Such assumption represents a limitation in the proposed model, since suppression of downstream mediators may not occur concurrently to COX-2 itself.

The model represented by equations (1)–(4) was selected from the data from experiment I and was used to describe the data in experiment II using the visual predictive check. Finally, all model parameters were re-estimated using all LT data obtained from the two experiments.

Statistical analysis

Results from experiments I and II after injection of saline or carrageenan in the control and treated groups with lumiracoxib are shown as mean data with their corresponding standard deviations. One-way analysis of variance, followed by Tukey's test was used to compare differences between treatments. Statistical significance was considered to be achieved when $P < 0.05$.

Materials

Lumiracoxib was provided by Novartis Farmacéutica, S.A. (Mexico City, Mexico). Naproxen was supplied by Grupo Roche-Syntex de México S.A. (Mexico City, Mexico). Carrageenan was purchased from Sigma Chemical Co. (St. Louis, MO, USA). Methanol, chromatographic grade, was purchased from Merck (Darmstadt, Germany). All other reagents and solvents used were purchased from commercial sources and were of analytical grade.

Results

Data description

Figure 2 shows the mean time profiles obtained from experiments I and II. In the upper panel, the observed PK profiles are represented. Maximum concentrations of lumiracoxib in plasma appeared within the two first hours after drug administration, with mean values of 0.33 ± 0.02, 0.94 ± 0.12, 1.45 ± 0.16 and 3.64 ± 0.25 $\mu g \cdot mL^{-1}$ for the 1, 3, 10 and 30 $mg \cdot kg^{-1}$ dose groups, respectively, suggesting dose-dependent pharmacokinetics.

All groups showed mean baseline LT ranging between 12 and 17 s (Figure 2, middle and lower panels), and a statistical analysis did not provide significant differences at baseline between groups I and IX ($P > 0.05$). The injection of saline

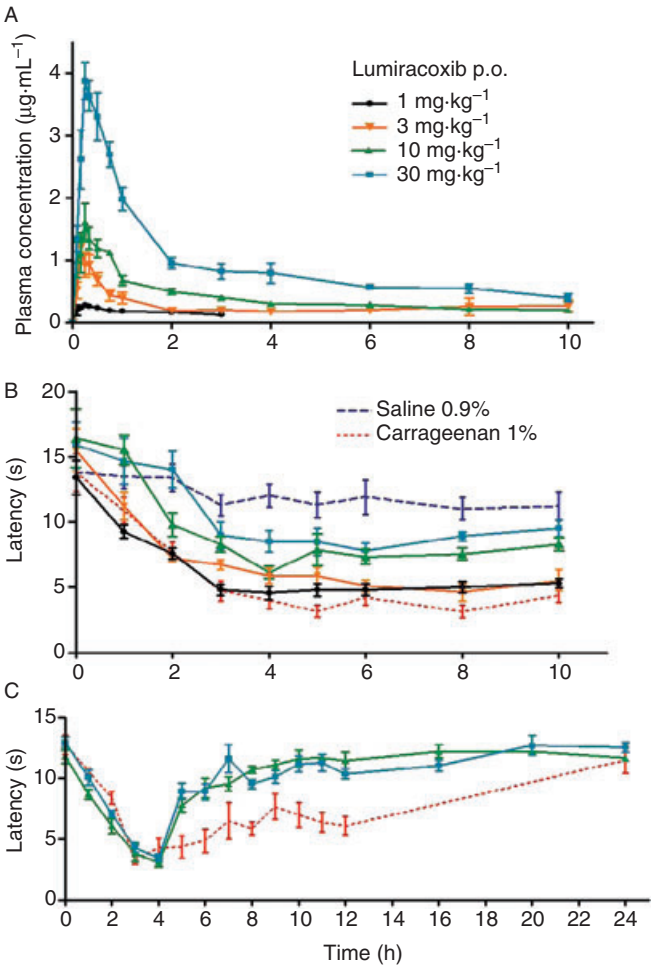

Figure 2 Time course of plasma concentrations of lumiracoxib (panel A). Time course of the latency response versus time profiles obtained from experiment I and II, panels B and C respectively. In panels B and C, data from rats injected with saline (control) or with carrageenan only (CG) are shown, as well as data from rats given carrageenan and the range of doses of lumiracoxib shown in panel A. Data are expressed as the mean + SD.

elicited a slight but significant decrease in the LT response compared with the baseline LT ($P < 0.05$). Injection of carrageenan produced a significant decrease in LT reaching the maximum at 3 h after injection ($P < 0.05$). In the case of experiment II, it can be observed that after 24 h, the LT response returned to its original value.

Lumiracoxib exerted a dose-dependent effect. The profiles shown in the middle panel of Figure 2 suggest that the two lowest doses (1 and 3 $mg \cdot kg^{-1}$) were not high enough to revert significantly the carrageenan-induced hyperalgesia ($P > 0.05$). On the other hand, the doses of 10 and 30 $mg \cdot kg^{-1}$ elicited significant antinociceptive response ($P < 0.05$).

Pharmacokinetic modelling

Disposition of lumiracoxib in plasma was best described by a two-compartment model. This model behaved significantly better that the one-compartment model ($P < 0.01$), and the three-compartment model did not show a significant

improvement ($P > 0.05$) over the selected model. The data allowed the estimation of IIV in V_c, the apparent volume of the central compartment, and *CL*, total plasma elimination clearance ($P < 0.01$).

A first-order rate of absorption model including a lag time (T_{lag}) was found an adequate model to describe the absorption process. IIV was also estimated for the first-order rate of absorption (K_A) and F_{rel} ($P < 0.01$).

Table 1 Parameter estimates from the final population pharmacokinetic model

Parameter	*Estimate*	*IIV (%)*
CL ($L \cdot h^{-1}$)	0.16 (14)	36 (43)
V_c (L)	0.49 (9)	39 (27)
Q ($L \cdot h^{-1}$)	0.42 (12)	–
V_T (L)	0.99 (19)	–
k_A (h^{-1})	15.2 (23)	92 (30)
T_{lag} (h)	0.06 (10)	–
$F_{rel} = 1 - I_{MAX} \times \left[\frac{D}{D + D_{50}}\right]$	I_{MAX} 0.67 (6) D_{50} ($mg \cdot kg^{-1}$) 4.3 (43)	18 (60)
Residual error		
Additive ($\mu g \cdot mL^{-1}$)	0.037 (20)	–
Proportional (%)	22 (10)	–

Parameter estimates are listed together with the coefficient of variation [CV (%)] in parenthesis.
CL, apparent plasma clearance; D_{50}, dose of lumiracoxib eliciting a decrease in F_{rel} equal to half of I_{MAX}; F_{rel}, relative bioavailability; IIV, inter-individual variability, is expressed as CV (%); I_{MAX}, maximum fractional reduction in F_{rel} that the dose level of lumiracoxib (D) can exert; V_c and V_T, apparent volumes of distribution of the central and peripheral compartments respectively; Q, inter-compartmental clearance; K_A, first-order rate constant of absorption; T_{lag}, lag time.

Dose showed statistical significant effects on F_{rel} ($P < 0.01$) but not on the other PK model parameters ($P > 0.05$). An increase in the administered dose was associated with a decrease in F_{rel}. The relationship between F_{rel} and dose was incorporated in the model using the expression represented in Table 1. The model predicts a maximum dose-elicited decrease in F_{rel} of approximately 30%.

The estimates of the selected model are listed in Table 1. Results indicate that parameters were estimated in general with good precision. Individual observations corresponding to three rats in each dose group are represented in Figure 3, together with their individual model predicted profiles, where it can be observed that the predictions from the model matches the observed data very well. Supplementary information (Figure S1) shows several goodness of fit plots obtained from the selected PK model. Those plots indicate that model mis-specifications are minor.

Selection of the final model was further supported by the predictive checks. In Table 2, the results from the numerical predictive check are listed. With the exception of C_{MAX} for the 3 $mg \cdot kg^{-1}$ dose group, the rest of mean values calculated from the raw data fall within the 2.5th–97.5th percentiles of the model-based simulated data.

Pharmacokinetic/pharmacodynamic modelling

The indirect response model accurately characterized the analgesic profiles following administration of lumiracoxib. For example, Figure 4 shows the results for the visual predictive check (lines in red) obtained from the model developed

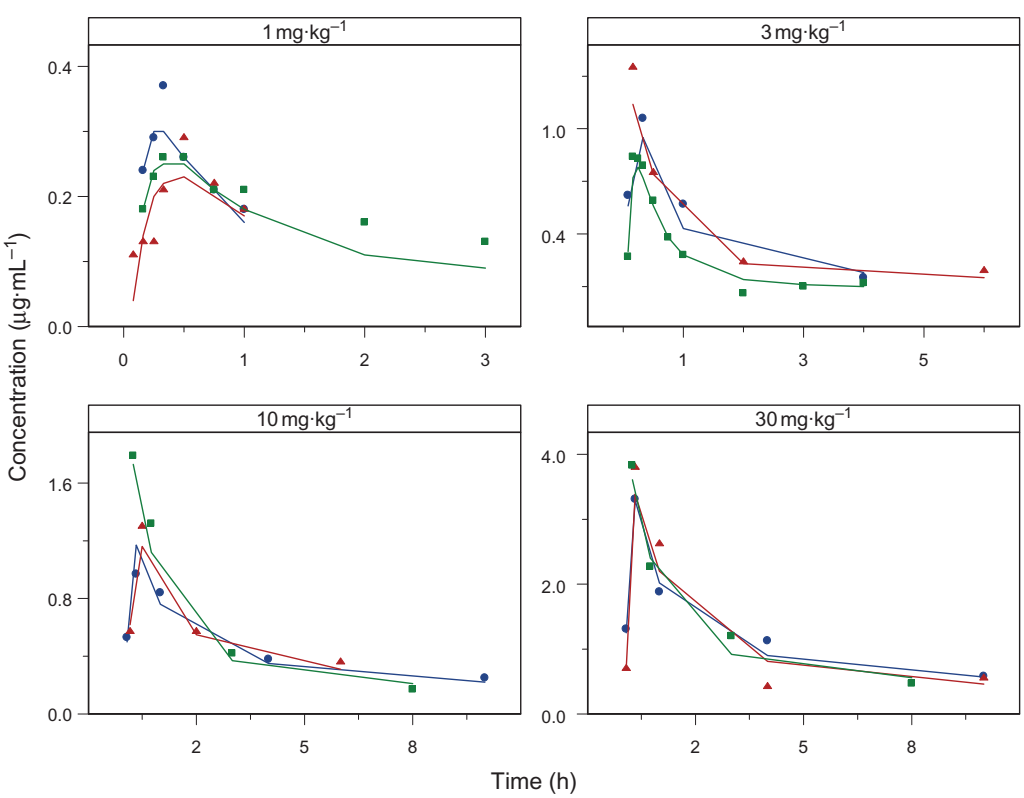

Figure 3 Individual lumiracoxib plasma concentrations versus time profiles from three rats. The symbols represent the individual raw data, and the lines, the predictions from the model.

Table 2 Results from the predictive check obtained from 1000 simulated studies based on the selected population pharmacokinetic model

Dose (mg·kg^{-1})	*C_{MAX} (μg·mL^{-1})*		*AUC_{0-last} (mg × h × L^{-1})*	
	Observed	*Simulated*	*Observed*	*Simulated*
1	0.33	0.31 [0.26–0.38]	0.2	0.18 [0.15–0.22]
3	0.94	0.68 [0.56–0.80]	1.23	0.94 [0.84–1.04]
10	1.45	1.65 [1.35–2.0]	3.63	3.7 [3.31–4.12]
30	3.64	3.94 [3.23–4.63]	9.4	8.7 [7.82–9.61]

Data in the table are expressed as means, with 2.5th and 97.5th percentiles in brackets.
AUC_{0-last}, area under the plasma concentration curve calculated from time 0 to last pharmacokinetic measurement time; C_{MAX}, maximum plasma concentration.

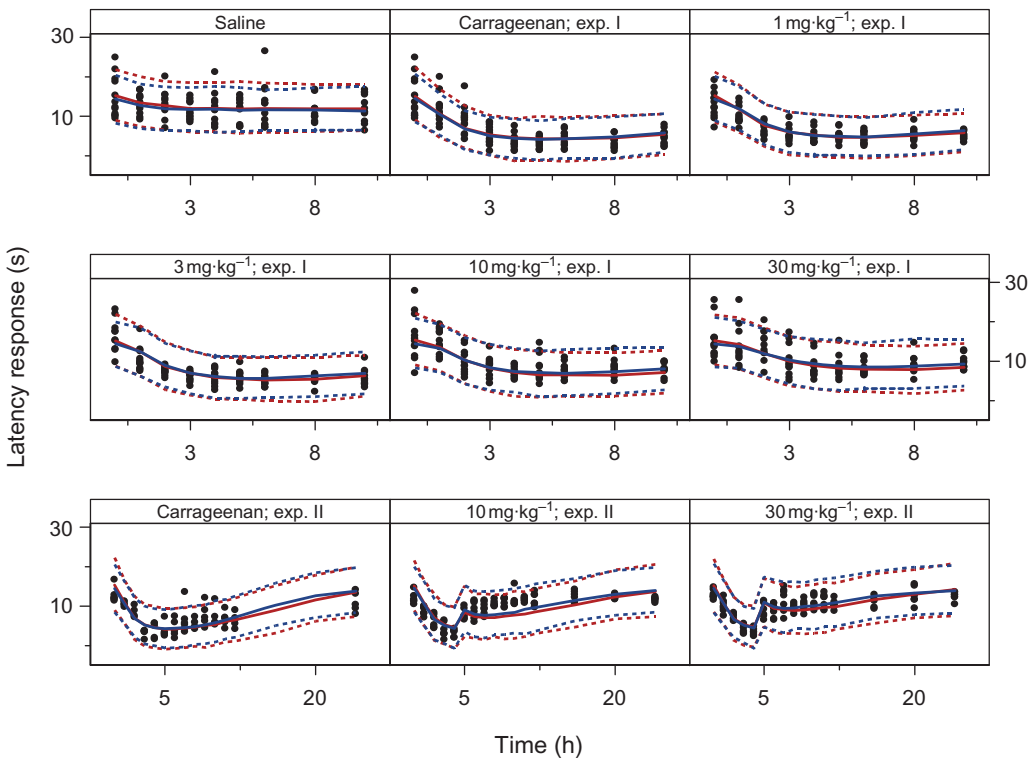

Figure 4 Results from the visual predictive check corresponding to the pharmacokinetic/pharmacodynamic model selected based on data from experiment I (profiles in red) and experiments I and II (profiles in blue). Lines correspond to the percentiles calculated from 1000 simulated time profiles (solid, 50th; dashed, 2.5 and 97.5th). The filled circles represent the observed data.

with the data from experiment I, where all groups (including those from experiment II) are described properly. Model parameter estimates are listed in Table 3 (middle columns). LT response data supported the inclusion of IIV on LT_0 and K_D only ($P < 0.01$), and not in the rest of the model parameters ($P > 0.05$).

During the model development process, the incorporation of an effect compartment (Sheiner *et al.*, 1979) accounting for the delay in lumiracoxib distribution between the central and the effect compartment was not supported by the data ($P > 0.05$). The assumption of reversible inhibition of $k_{S\_COX\text{-}2(t)}$ increased the minimum value of the objective function by eight points for the same number of parameters, indicating a worse fit. Therefore, the model structure was based on a reversible competition between lumiracoxib and arachidonic acid for the binding to COX-2 (equation 4). In addition, the inclusion of a sigmoidicity parameter in equation 4 was not statistically significant ($P > 0.05$).

The dynamics of the synthesis of the unobserved COX-2 during the period of the experiments was evaluated in detail, fitting both time-constant and time-variant models to the data. Other models fitted to the data to describe the course of $k_{S\_COX\text{-}2_{(t)}}$ (i.e. linear or exponential decay with time) described the observations significantly worse than the selected model using the gamma function (equation 3) ($P < 0.01$). For the case of group I, where only saline was injected, data suggested a constant rate of synthesis; however, for those groups of animals receiving carrageenan, the model represented by equation 2 was significantly better ($P < 0.01$).

When all LT response data from experiments I and II were pooled and analysed together, parameter estimates remained almost unchanged, but their precision was improved (Table 3, right column).

Individual observations corresponding to two rats in each dose group are represented in Figure 5 together with their individual model predicted profiles, where it can be observed

that the model describes the data very well. Supplementary information (Figure S2) shows several goodness of fit plots obtained from the selected model. Those plots indicate that model mis-specifications are minor.

Selection of the final model was further supported by the predictive checks. Figure 4 represents also the results from the visual predictive check (lines in blue) corresponding to the model and parameter estimates obtained from the simultaneous fit of data from experiment I and II. It can be seen that the model describes properly both, the mean tendency and the dispersion in the data for all the dose groups, and that model predictions obtained from the two sets of parameters listed in Table 3 are almost indistinguishable.

In Table 4, the results from the numerical predictive check are listed. With the exception of Red_{MAX}(%) for the 1 mg·kg^{-1} dose group, the rest of mean values calculated from the raw data fall within the 2.5th–97.5th percentiles of the model-based simulated data.

Figure 6 shows, in the left panel, the typical model predicted time profiles of COX-2 in group I and in groups which received carrageenan. The right-hand panel in Figure 6 represents the concentration versus effect relationship for lumiracoxib reflected in equation 4 and corresponds to an estimate of K_D of 0.24 µg·mL^{-1} (Table 3).

Table 3 Parameter estimates from the final population pharmacodynamic models selected by experiment I and experiment I and II

Parameter	*Experiment I*		*Experiment I and II*	
	Estimate	*IIV (%)*	*Estimate*	*IIV (%)*
$k_{S\_COX\text{-}2}$ (COX-2·h^{-1})[a]	0.20 (62)	–	0.21 (38)	–
A (COX-2·h^{-2})	1.32 (24)	–	1.42 (15)	–
α	1.07 (29)	–	1.3 (21)	–
β (h^{-1})	0.27 (22)	–	0.33 (17)	–
$k_{D\_COX\text{-}2}$ (h^{-1})	0.72 (68)	–	0.89 (39)	–
K_D (µg·mL^{-1})	0.33 (24)	33 (126)	0.24 (21)	62 (54)
LT_0 (s)	15.1 (3)	13 (28)	14.3 (3)	13 (33)
Residual error (s)	2.6 (9)	–	2.4 (10)	–

Parameter estimates are listed together with the coefficient of variation [CV (%)] in parenthesis. IIV, inter-individual variability, is expressed as CV (%); $k_{S\_COX\text{-}2_{(t)}}$ and $k_{D\_COX\text{-}2}$ represent the synthesis and degradation processes of the enzyme COX-2. *A*, α and β are the parameters of the gamma function describing the time course and intensity of the COX-2 synthesis rate in the groups injected with carrageenan. K_D is the equilibrium dissociation constant of the COX-2-C_P complex, where C_P, is refers to the concentration of lumiracoxib in plasma. LT_0, paw withdrawal latency time at baseline.
[a]Estimate of $k_{S\_COX\text{-}2}$ corresponding to the group receiving saline.

Discussion and conclusions

In this work, a PK/PD model was developed for the antinociceptive effects of lumiracoxib in an animal model of hyperalgesia, fulfilling therefore the primary objective of the current study.

The plantar test has been used to assess the hindpaw nociceptive withdrawal latencies to thermal stimuli in rats (Hargreaves *et al.*, 1988). This test is a simple, rapid and sensitive method suitable for detecting peripheral hyperalgesia in rats (Hargreaves *et al.*, 1988). Despite differences in the response to different classes of pharmacological agents, this

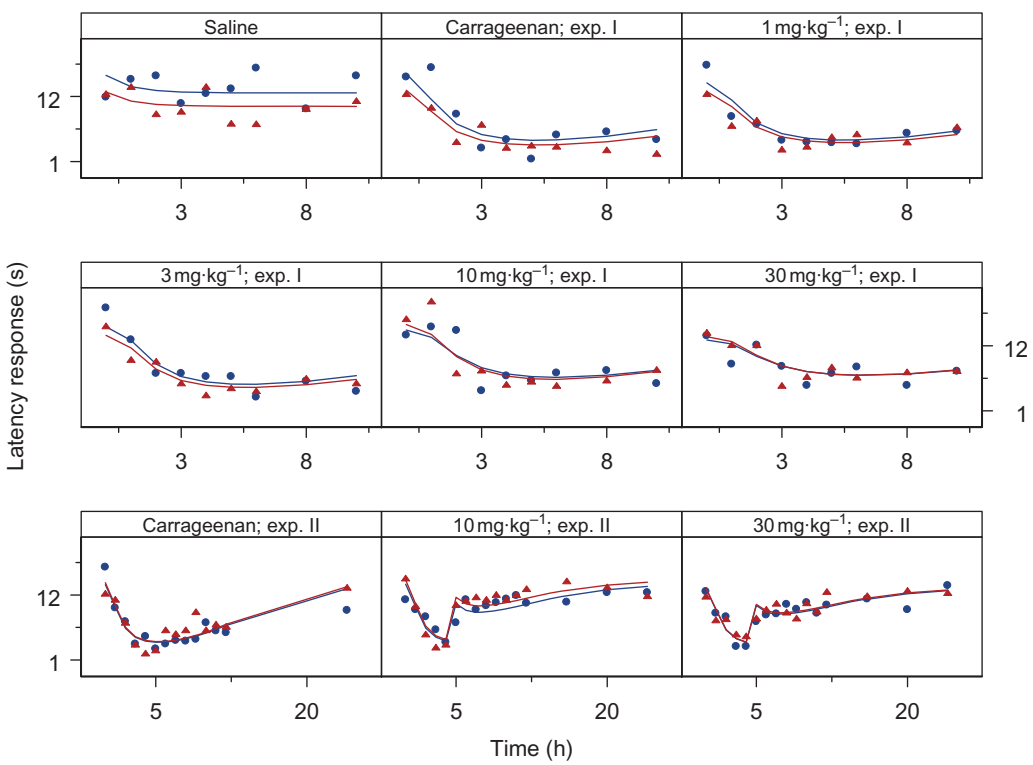

Figure 5 Individual latency response versus time profiles from two rats. The symbols represent the individual raw data and the lines, the predictions from the model.

Table 4 Results from the predictive check obtained from 1000 simulated studies based on the selected population pharmacokinetic/pharmacodynamic model

Dose (mg·kg^{-1})	LT_{MIN} *(s)*		Red_{MAX} *(%)*	
	Observed	*Simulated*	*Observed*	*Simulated*
Saline	8.1	8.3 [7.4–9.4]	45	42.5 [38–48]
Carrageenan[a]	1.9	1.6 [0.8–2.4]	87	89 [84–95]
1	3.3	2.3 [1.5–3.2]	75	84 [78–89]
3	3.9	3.05 [2.2–4]	76	79 [73–86]
10	5.3	4.4 [3.2–5.6]	67	70 [63–77]
30	6.5	6 [4.9–7.1]	57	58 [52–66]
10[b]	3	2.6 [1.5–3.8]	73	82 [75–90]
30[b]	3.5	3 [1.8–4.3]	73	79 [71–88]

Data in the table are expressed as means, with 2.5th and 97.5th percentiles in brackets.
[a]Data from experiment I and II combined.
[b]Dose groups corresponding to experiment II.
LT_{MIN}, minimum latency response; Red_{MAX}, maximum percentage reduction in latency response with respect to baseline.

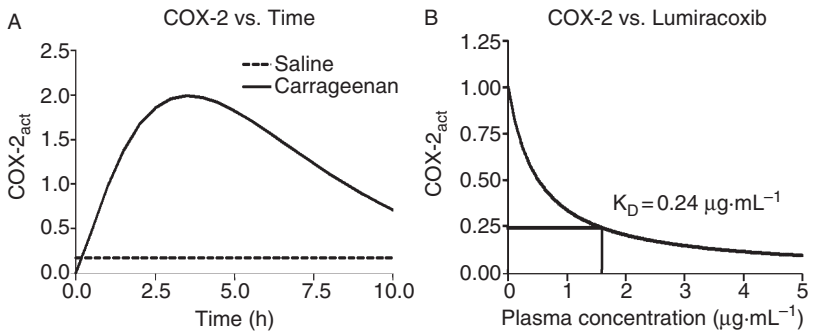

Figure 6 Left panel: typical model-predicted time course of COX-2 after saline and carrageenan injection. Right panel: pharmacodynamic relationship between $COX\text{-}2_{\_act}$ and lumiracoxib plasma concentration.

end point is clearly sensitive to the COX-2 selective inhibitor lumiracoxib.

As it can be appreciated in Figures 2 and 4, lumiracoxib was not able to completely reverse carrageenan-induced hyperalgesia. That result, however, should be expected if the hyperalgesic response was solely due to the mediators produced by COX-2. It is now known that in several models of inflammation in the rat, platelet COX-1 activity can be a source of inflammatory mediators, such as PGE_2 (Giuliano and Warner, 2002). Moreover, Wallace *et al.* (1998; 1999) have reported that certain COX-2 inhibitors need to be administered at non-selective, COX-1-inhibiting doses to abolish the inflammatory response in the carrageenan-induced paw-oedema or the air pouch model. As lumiracoxib is extremely selective for COX-2, it is unlikely that platelet COX-1 activity was affected at the doses used in our study. Hence, lumiracoxib produces only a partial inhibition of the hyperalgesic response.

Pharmacokinetic model

In the present study, a two-compartmental model was selected, which is consistent with previous preclinical results, where the PK of lumiracoxib was investigated (Esser *et al.*, 2005a). A high bioavailability was assumed, which is a reasonable assumption given the fact that the drug was administered as a suspension, and the low estimated clearance. Rordorf *et al.* (2005) reported a value of 0.74 for the absolute bioavailability in humans when lumiracoxib was administered in tablets.

Relative bioavailability was found to be dose dependent, with a typical value for the highest dose administered ~30% lower than the corresponding to the lowest dose level studied. Similar results were found by Rordorf *et al.* (2005) in humans, where the C_{MAX} did not increase proportionally with the increase in dose. It is also worth noting that a very similar finding has been seen for the NSAID naproxen (Josa *et al.*, 2001). It is difficult to provide a mechanism explaining the dose-dependent decrease in relative bioavailability given the data available. This could be due to the limited solubility of the drug, but further investigation is required to fully elucidate this issue.

COX-2 model

Intra-plantar injection of carrageenan induces a transient increase in COX-2 activity. Seibert *et al.* (1994) and Nantel *et al.* (1999) reported that COX-2 mRNA was just detectable within 60 min, with a substantial induction observed at 3 h after injection of carrageenan in the paw. In the current evaluation, the (unobserved) time course of COX-2 activity was modelled empirically using the gamma function used by Giraudel *et al.* (2005) to describe the effects of meloxicam in

an inflammation model in cats. Interestingly, the estimates of the gamma function reported by us are of the same order than those shown by Giraudel *et al.* (2005), and provided a very good description of the control groups. The typical COX-2 profile shown in Figure 6 (right panel) resembled very closely the experimental data reported by Seibert *et al.* (1994) and Jain *et al.* (2008).

Pharmacodynamic model

It is well known that selective COX-2 inhibitors exert their pharmacological action through a reversible inhibition of COX-2, hampering the formation of the COX-2-arachidonic acid complex and therefore decreasing the synthesis of inflammatory mediators, such as prostaglandins (Vane, 1971). However, and to the best of our knowledge, previous studies on the PK/PD modelling of the effects of NSAIDs incorporate the drug action as an inhibition (INH) of the synthesis rate of inflammation mediators (k_{in}), (Trocóniz *et al.*, 2000; Josa *et al.*, 2001; Giraudel *et al.*, 2005) as follows: $dR/dt = k_{in} \times INH - \underline{k}_{out} \times R$, where dR/dt is the rate of change of inflammation mediators or the measured response (R), and k_{out} being the first-order rate of degradation.

The model selected in the current study resembled better the known mechanism of action of the NSAIDs, as the drug does not affect the rate of synthesis of COX-2, but competes reversibly with arachidonic acid for binding to COX-2. The selected model provided a better fit to the data in comparison to the rate inhibition model, and described the time course of the latency response in all the dose groups. It should be taken into account that the pharmacodynamic model used in this analysis is based on the receptor occupancy theory and assumes a linear transduction function, which might not be the case, as it has been shown when the operational model of agonism (Black and Leff, 1983) has been applied to different classes of drugs (Van der Graaf *et al.*, 1997; 1999). The data available in this work do not support the investigation of more complex pharmacodynamic models, which requires the integration of information obtained from different compounds of the same class (Van der Graaf and Danhof, 1997).

The estimates obtained for the pharmacodynamic parameters are difficult to compare across different studies because of the different designs and different types of measured response, and the lack of PK/PD results for this particular drug. The estimate obtained for K_D 0.24 $\mu g \cdot mL^{-1}$ (0.81 μM), is too high compared with results obtained from *in vitro* binding experiments, where IC_{50} has been estimated to be 17 $ng \cdot mL^{-1}$ (60 nM) (Esser *et al.*, 2005b). It should be noted that the IC_{50} values reported in the literature refer only to the inhibition of PGE_2 production by lumiracoxib (Esser *et al.*, 2005a,b; Rordorf *et al.*, 2005). COX-2, however, does not only produce PGE_2 and other prostaglandins. COX-2 activity results in the synthesis of a variety of mediators involved in the hyperalgesic response. This is why we preferred to express the products of COX-2 as MED. MED refers to all the mediators generated by COX-2 activity involved in the hyperalgesic response. Thus, our K_D value refers to total COX-2 activity, and not only to PGE_2 production.

Notwithstanding, it should be noted that the *in vivo* situation is considerably different from that *in vitro*. Our K_D estimates correspond to total lumiracoxib plasma concentration. It is known that lumiracoxib is bound extensively (about 98%) to human plasma proteins (Rordorf *et al.*, 2005). There is evidence that plasma protein binding is similar in several mammalian species, including human, monkey and rat (MHRA Medicines and Healthcare Products Regulatory Agency, 2005). Thus, considering the unbound lumiracoxib concentration, the K_D value is 16 nM, being in the range of previously reported values *in vitro*.

It has been reported that lumiracoxib is not only a COX-2 inhibitor, as it also exhibits activity as a thromboxane receptor antagonist in the micromolar concentration range (Selg *et al.*, 2007). There is evidence that thromboxane receptors are involved in inflammation (Thomas *et al.*, 2003) and could contribute to nociception (Evans *et al.*, 2000) in certain assays. Nonetheless, to our knowledge, there is no available evidence that thromboxane receptors play a role in the Hargraves model of thermal hyperalgesia. Therefore, we preferred to limit our pharmacodynamic model to lumiracoxib actions on COX-2, which explain reasonably well the experimental data.

It has been shown that the metabolite 4′-hydroxy-lumiracoxib exhibits pharmacological activity *in vitro*, having similar potency and COX-2 selectivity to the parent molecule (Mangold *et al.*, 2004). Notwithstanding, plasma concentrations of 4′-hydroxy-lumiracoxib *in* vivo are much lower than those of lumiracoxib (Rordorf *et al.*, 2005). Those findings, together with the fact that no dose dependency was found for the K_D parameter in the current study, suggest that, under the experimental conditions used in the current study, the role of 4′-hidroxy-lumriacoxib on the analgesic effects is negligible.

The robustness of the model was confirmed both by the accuracy of the estimates for latency response when lumiracoxib was administered at the time of maximum rate of synthesis of COX-2 and by predictions of the latency response beyond the experimental window in experiment I.

In conclusion, the use of PK/PD modelling enables accurate assessment of the analgesic response, taking into account the underlying pharmacological mechanisms. As illustrated for lumiracoxib, this approach yields parameters describing drug properties in a dose-independent manner. It is anticipated that PK/PD modelling can provide a more robust rationale for dose selection of COX-inhibitors in humans.

Acknowledgements

We thank Q.F.B. Martha Patricia Gonzáles García for her technical support. Dalia Angélica Vásquez Bahena is a CONACyT fellow with Grant number 207023.

Conflict of interests

None.

References

Ahuja N, Singh A, Singh B (2003). Rofecoxib: an update on physicochemical, pharmaceutical, pharmacodynamic and pharmacokinetic aspects. *J Pharm Pharmacol* **55**: 859–894.

Beal SL, Sheiner LB (1982). Estimating population kinetics. *CRC Crit Reviews in Bioengineering* **8**: 195–222.

Beal SL, Sheiner LB (1989–2006). *NONMEM Users Guides*. GloboMax, Inc.: Hanover, MD.

Black JW, Leff P (1983). Operational models of pharmacological agonism. *Proc R Soc Lond B* **220**: 141–162.

Bombardier C, Laine L, Reicin A, Shapiro D, Burgos-Vargas R, Davis B *et al*. (2000). Comparison of upper gastrointestinal toxicity of rofecoxib and naproxen in patients with rheumatoid arthritis. VIGOR Study Group. *N Engl J Med* **343**: 1520–1528.

Castañeda-Hernández G, Favari L, Hoyo-Vadillo C (1995). Relationship between naproxen plasma concentration and its anti-inflammatory effect in experimental hepatitis. *Arzneim-Forsch/Drug Res* **45**: 585–589.

Crofford LJ (1997). COX-1 and COX-2 tissue expression: implications and predictions. *J Rheumatol Suppl* **49**: 15–19.

Cruz L, Castañeda-Hernández G, Flores-Murrieta FJ, García-López P, Guízar-Sahagún G (2002). Alteration of phenacetin pharmacokinetics after experimental spinal cord injury. *Proc West Pharmacol Soc* **45**: 4–5.

Dayneka NL, Garg V, Jusko WJ (1993). Comparison of four basic models of indirect pharmacodynamic responses. *J Pharmacokinet Biopharm* **21**: 457–478.

Esser R, Berry C, Du Z, Dawson J, Fox A, Fujimoto RA *et al*. (2005a). Preclinical pharmacology of lumiracoxib: a novel selective inhibitor of cyclooxygenase-2. *Br J Pharmacol* **144**: 538–550.

Esser RE, Miserendino-Molteni R, Sharr M, Zhang X, Porter W, Ramos L *et al*. (2005b). Pharmacodynamic behaviour of the selective cyclooxygenase-2 inhibitor lumiracoxib in the lipopolysaccharide-stimulated rat air pouch model. *Eur J Pharm Sci* **25**: 25–30.

Evans AR, Junger H, Southall MD, Nicol GD, Sorkin LS, Broome JT *et al*. (2000). Isoprostanes, novel eicosanoids that produce nociception and sensitize rat sensory neurons. *J Pharmacol Exp Ther* **293**: 912–920.

Flores-Murrieta FJ, Ko HC, Flores-Acevedo DM, López-Muñoz FJ, Jusko WJ, Sale ME *et al*. (1998). Pharmacokinetic-pharmacodynamic modelling of tolmetin antinociceptive effect in the rat using an indirect response model: a population approach. *J Pharmacokinet Biopharm* **26**: 547–557.

Fu JY, Masferrer JL, Seibert K, Raz A, Needleman P (1990). The induction and suppression of prostaglandin H2 synthase (cyclooxygenase) in human monocytes. *J Biol Chem* **265**: 16737–16740.

Giraudel JM, Diquelou A, Laroute V, Lees P, Toutain PL (2005). Pharmacokinetic/pharmacodynamic modelling of NSAIDs in a model of reversible inflammation in the cat. *Br J Pharmacol* **146**: 642–653.

Giuliano F, Warner TD (2002). Origins of prostaglandin E2: involvements of cycloosygenase (COX)-1 and COX-2 in human and rat systems. *J Pharmacol Exp Ther* **303**: 1001–1006.

Goldstein JL, Correa P, Zhao WW, Burr AM, Hubbard RC, Verbug KM *et al*. (2001). Reduced incidence of gastroduodenal ulcers with celecoxib, a novel cyclooxygenase-2 inhibitor, compared to naproxen in patients with arthritis. *Am J Gastroenterol* **96**: 1019–1027.

Hargreaves K, Dubner R, Brown F, Flores C, Joris J (1988). A new and sensitive method for measuring thermal nociception in cutaneous hyperalgesia. *Pain* **32**: 77–88.

Hernández-Díaz S, García-Rodríguez LA (2001). Epidemiologic assessment of the safety of conventional nonsteroidal anti-inflammatory drugs. *Am J Med* **110** (Suppl. 3A): 20S–27S.

Hinz B, Brune K (2008). Can drug removals involving cyclooxygenase-2 inhibitors be avoided? A plea for human pharmacology. *Trends Pharmacol Sci* **29**: 391–397.

Huntjens DR, Danhof M, Della Pasqua OE (2005). Pharmacokinetic-pharmacodynamic correlations and biomarkers in the development of COX-2 inhibitors. *Rheumatology* **44**: 846–859.

Jain NK, Ishikawa TO, Spigelman I, Herschman HR (2008). COX-2 expression and function in the hyperalgesic response to paw inflammation in mice. *Prostaglandins Leukot Essent Fatty Acids* **79**: 183–190.

Jonsson EN, Karlsson MO (1999). Xpose – an Splus based population pharmacokinetic/pharmacodynamic model building aid for NONMEM. *Comput Methods Programs Biomed* **58**: 51–64.

Josa M, Urizar JP, Rapado J, Dios-Viéitez C, Castañeda-Hernández G, Flores-Murrieta F *et al*. (2001). Pharmacokinetic/pharmacodynamic modelling of antipyretic and anti-inflammatory effects of naproxen in the rat. *J Pharmacol Exp Ther* **297**: 198–205.

Karlsson MO, Holford NH (2008). A tutorial on Visual Predictive Checks. Page 17 (2008= Abstract 1434). Available at: http://www.page-meeting.org/?abstract=1434 (accessed 24 September 2009).

Kellstein D, Ott D, Jayawardene S, Fricke J (2004). Analgesic efficacy of a single dose of lumiracoxib compared with rofecoxib, celecoxib and placebo in the treatment of post-operative dental pain. *Int J Clin Pract* **58**: 244–250.

Mangold JB, Gu H, Rodriguez LC, Bonner J, Dickson J, Rordorf C (2004). Pharmacokinetics and metabolism of lumiracoxib in healthy male subjects. *Drug Metab Dispos* **32**: 566–571.

MHRA Medicines and Healthcare products Regulatory Agency (2005). UK Public Assessment Report for Prexige 100 mg tablets (Lumiracoxib) PL 00101/0677. Available at: http://www.mhra.gov.uk/home/idcplg?IdcService=GET_FILE&dDocName=con2022707&RevisionSelectionMethod=Latest (accessed 24 July 2009).

Mysler E (2004). Lumiracoxib (Prexige®): a new selective COX-2 inhibitor. *Int J Clin Pract* **58**: 606–611.

Nantel F, Denis D, Gordon R, Northey A, Cirino M, Metters KM *et al*. (1999). Distribution and regulation of cyclooxygenase-2 in carrageenan-induced inflammation. *Br J Pharmacol* **128**: 853–859.

Ortiz MI, Castañeda-Hernández G (2008). Examination of the interaction between peripheral lumiracoxib and opioids on the 1% formalin test in rats. *Eur J Pain* **12**: 233–241.

Rordorf CM, Choi L, Marshall P, Mangold JB (2005). Clinical pharmacology of lumiracoxib: a selective cyclo-oxygenase-2 inhibitor. *Clin Pharmacokinetic* **44**: 1247–1266.

Scott G, Rordorf C, Reynolds C, Kalbag J, Looby M, Milosavljev S *et al*. (2004). Pharmacokinetics of lumiracoxib in plasma and synovial fluid. *Clin Pharmacokinet* **43**: 467–478.

Seibert K, Zhang Y, Leahy K, Hauser S, Masferrer J, Perkins W *et al*. (1994). Pharmacological and biochemical demonstration of the role of cyclooxygenase 2 in inflammation and pain. *Proc Natl Acad Sci USA* **91**: 12013–12017.

Selg E, Buccellati C, Andersson M, Rovati GE, Ezinga M, Sala A *et al*. (2007). Antagonism of thromboxane receptors by diclofenac and lumiracoxib. *Br J Pharmacol* **152**: 1185–1195.

Sheiner LB, Ludden TM (1992). Population pharmacokinetics/dynamics. Ann Rev. *Pharmacol Toxicol* **32**: 185–209.

Sheiner LB, Stanski DR, Vozeh S, Miller RD, Ham J (1979). Simultaneous modelling of pharmacokinetics andpharmacodynamics: application to *d*-tubocurarine. *Clin Pharmacol Ther* **25**: 358–371.

Shi S, Klotz U (2008). Clinical use and pharmacological properties of selective COX-2 inhibitors. *Eur Clin Pharmacol* **64**: 233–252.

Thomas DW, Rocha PN, Nataraj C, Robinson LA, Spurney RF, Koller BH *et al*. (2003). Proinflammatory actions of thromboxane receptors to enhance cellular immune responses. *J Immunol* **171**: 6389–6395.

Trocóniz IF, Armenteros S, Planelles MV, Bennie J, Calvo R, Domínguez R (2000). Pharmacokinetic-pharmacodynamic modelling of the antipyretic effect of two oral formulations of ibuprofen. *Clin Pharmacokinet* **38**: 505–518.

Van Der Graaf PH, Danhof M (1997). Analysis of drug-receptor interactions in vivo: a new approach in pharmacokinetic-pharmacodynamic modelling. *Int J Clin Pharmacol Ther* **35**: 442–446.

Van Der Graaf PH, Van Schaick EA, Math-ot RA, Ijzerman AP, Danhof M (1997). Mechanism-based pharmacokinetic-pharmacodynamic modelling of the effects of N6-cyclopentyladenosine analogs on heart rate in rat: estimation of in vivo operational affinity and efficacy at adenosine A1 receptors. *J Pharmacol Exp Ther* **283**: 809–816.

Van der Graaf PH, Van Schaick EA, Visser SA, De Greef HJ, Ijzerman AP, Danhof M (1999). Mechanism-based pharmacokinetic-pharmacodynamic modelling of antilipolytic effects of adenosine A(1) receptor agonists in rats: prediction of tissue-dependent efficacy in vivo. *J Pharmacol Exp Ther* **290**: 702–709.

Vane JR (1971). Inhibition of prostaglandin synthesis as a mechanism of action of aspirin-like drugs. *Nat New Biol* **231**: 232–235.

Wallace JL, Bak A, McKnight W, Asfaha S, Sharkey KA, MacNaughton WK (1998). Cyclooxygenase 1 contributes to inflammatory responses in rats and mice: implications for gastrointestinal toxicity. *Gastroenterology* **115**: 101–109.

Wallace JL, Chapman K, McKnight W (1999). Limited anti-inflammatory efficacy of cyclo-oxygenase-2 inhibition in carrageenan-airpouch inflammation. *Br J Pharmacol* **126**: 1200–1204.

Warner TD, Giuliano F, Vojnovic I, Bukasa A, Mitchell JA, Vane JR (1999). Nonsteroid drug selectivities for cyclo-oxygenase-1 rather than cyclo-oxygenase-2 are associated with human gastrointestinal toxicity: a full in vitro analysis. *Proc Natl Acad Sci USA* **9**: 7563–7568.

Weaver ML, Flood DJ, Kimble EF, Fujimoto RA (2003). Lumiracoxib demonstrates preferential distribution to inflamed tissue in the rat following a single oral dose: an effect not seen with other cyclooxygenase-2 inhibitors. *Ann Rheum Dis* **62** (Suppl. 1): 378.

Wise ME (1985). Negative power functions of time in pharmacokinetics and their implications. *J Pharmacokinet Biopharm* **13**: 309–346.

Zimmermann M (1983). Ethical guidelines for investigations on experimental pain in conscious animals. *Pain* **16**: 109–110.

Supporting Information

Additional Supporting Information may be found in the online version of this article:

Figure S1 Goodness of fit plots corresponding to the selected population pharmacokinetic model. The solid lines represent the perfect fit (black) and a smooth through the data (grey).
Figure S2 Goodness of fit plots corresponding to the selected population pharmacokinetic/pharmacodynamic model. The solid lines represent the perfect fit (black) and a smooth through the data (grey).

Please note: Wiley-Blackwell are not responsible for the content or functionality of any supporting materials supplied by the authors. Any queries (other than missing material) should be directed to the corresponding author for the article.